Electronic Supplementary Information

Nitrile-containing copper(II) porphyrin coordination complexes for efficient anticancer activity and mechanism research

Qian Zhang, Jin-li Liu, Xiao-xia Feng* Jia-cheng Liu *

Key Laboratory of Eco-functional Polymer Materials of the Ministry of Education, Key Laboratory of Eco-environmental Polymer Materials of Gansu Province, Key Laboratory of Bioelectrochemistry & Environmental Analysis of Gansu Province, College of Chemistry and Chemical Engineering, Northwest Normal University, Lanzhou 730070, People's Republic of China

** Corresponding author.*

E-mail addresses: jcliu8@nwnu.edu.cn (J. C. Liu).

1. Experimental

1. 1. Materials

Penicillin/Streptomycin, MTT [3-(4, 5-dimethylthiazol-2-yl)-2, 5-diphenyltetrazolium bromide], Calf tymus DNA (ct-DNA), JC-1 mitochondrial membrane potential assay kit and RNaseA were purchased from Solarbio, DMEM-F12 medium, RPMI 1640 medium, DMEM (high glucose) medium were purchased from HyClone, Fetal bovine serum was purchased from Biological Industries, Calcein-AM/PI was purchased from Yeasen. All other chemicals were commercially analytical grade and were used without further purification. Human lung carcinoma cell lines A549 and H-1975, human liver carcinoma cell lines HepG2, human breast cancer cells T47D and breast cells Hs 578Bst were purchased from Chinese Academy of Sciences Shanghai Institute of Cell Bank.

1. 2. Instrumentation

Cell cycle analysis and assessment of intracellular mitochondrial membrane potential (MMP) were taken on a FACScan flow cytometer (Bection Dickinson, USA). Cell viability assay was performed with a microplate reader (model MK3, Thermo Fisher). Apoptosis detection by Calcein-AM/PI fluorescent staining and assessment of intracellular mitochondrial membrane potential (MMP) by JC-1 fluorescent staining were taken on fluorescent microscope (Olympus IX71). The Luminescence spectrum was measured by LS-55 (PEUSA Inc) fluorescence spectrophotometer at room temperature. UV-Vis spectra were taken on a UV-2550 spectrometer.

1. 3. Synthesis of sample

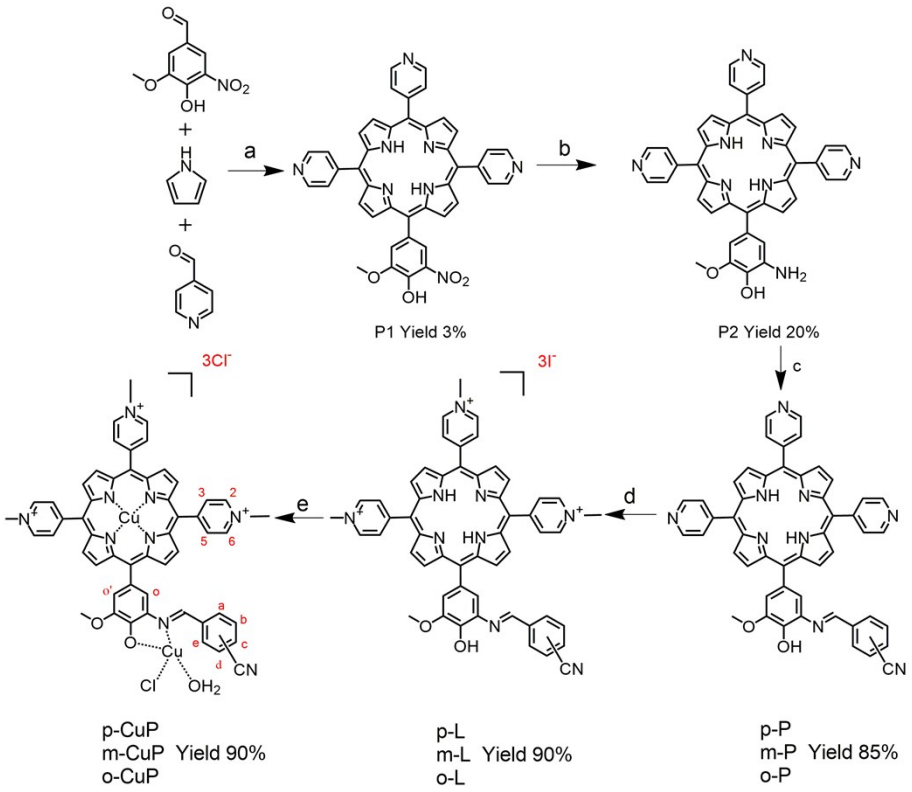

Scheme S1. The synthetic routes of Cu(II) complexes **p-CuP**, **m-CuP** and **o-CuP**. a. Propionic acid and propionic anhydride, 140 ℃ reflux 1.5 h; b. $SnCl_2 \cdot 2H_2O$, HCl (6 M), Ar, r. t, 15 h; c. p-Cyanobenzaldehyde (or m-Cyanobenzaldehyde or o-Cyanobenzaldehyde), toluene, acetic acid, 75 ℃, 72 h; d. CH_3I, Ar, DMF, 50 ℃, 3 h; e. $CuCl_2 \cdot 2H_2O$, MeOH, 60 ℃, 6 h;

1. 3. 1. Synthesis of P1 and P2

P1 and **P2** were prepared according to the method for our previous work [1].

1. 3. 2. Synthesis of p-P, m-P and o-P

The precursor porphyrin **P2** (100 mg, 0.15 mmol) and p-Cyanobenzaldehyde or m-Cyanobenzaldehyde or o-Cyanobenzaldehyde (20 mg, 0.15 mmol) were dissolved in toluene, a few drops of acetic acid were added. The solution was stirred 72h at 75 ℃ and washed with diethyl ether, then get the product **p-P** or **m-P** or **o-P** and 85% isolated yield.

p-P: ^{1}H NMR ($CDCl_3$, 600 MHz): -2.88 (s, 2H, NH-H), 4.02 (s, 3H, -OCH_3-H), 7.74, 7.76 (br, 2H, o, o'-ph-H), 7.80 (s, 1H, b-ph-H), 7.82, 7.83 (br, 1H, d-ph-H), 7.91 (s, 1H, CH=N-H), 8.03, 8.04 (d, J=6 Hz, 2H, a, e-ph-H), 8.16 (s, 6H, 3, 5 Py-H), 8.80-8.88 (m, 6H, 2, 6 Py-H), 9.04-9.06 (m, 8H, β-pyrrole-H). HRMS (ESI, positive ion mode, m/z): $[M+H]^+$ calcd for $[C_{50}H_{33}N_9O_2+H]^+$, 792.28300; found, 792.28308.

m-P: ^{1}H NMR ($CDCl_3$, 600 MHz): -2.86 (s, 2H, NH-H), 4.02 (s, 3H, -OCH_3-H), 7.53 (s, 1H, o-ph-H), 7.56-7.59 (m, 1H, o'-ph-H), 7.67 (s, 1H, a-ph-H), 7.74, 7.75 (br, 1H, c-ph-H), 7.78 (s, 1H, d-ph-H), 7.83 (s, 1H, e-ph-H), 8.03 (s, 1H, CH=N-H), 8.15 (s, 6H, 3, 5 Py-H), 8.75-8.85 (m, 6H, 2, 6 Py-H), 8.97-9.05 (m, 8H, β-pyrrole-H). HRMS (ESI, positive ion mode, m/z): $[M+H]^+$ calcd for $[C_{50}H_{33}N_9O_2+H]^+$, 792.28300; found, 792.28271.

o-P: ^{1}H NMR ($CDCl_3$, 600 MHz): -2.85 (s, 2H, NH-H), 4.02 (s, 3H, -OCH_3-H), 7.83-7.85 (m, 2H, o, o'-ph-H), 8.02 (m, 2H, b, c-ph-H), 8.04-8.06 (m, 2H, d, e-ph-H), 8.08, 8.10 (d, J=12 Hz, 1H, CH=N-H), 8.17-8.18 (m, 6H, 3, 5 Py-H), 8.80-8.86 (m, 6H, 2, 6 Py-H), 9.06-9.09 (m, 8H, β-pyrrole-H). HRMS (ESI, positive ion mode, m/z): $[M+H]^+$ calcd for $[C_{50}H_{33}N_9O_2+H]^+$, 792.28300; found, 792.28253.

1. 3. 3. Synthesis of p-L, m-L and o-L

In 5 ml DMF was added 100 mg (0.13mmol) **p-P** or **m-P** or **o-P** an excess of iodomethane under argon in the dark, after the solution was stirred at 75 ℃ for 72h and was washed with CH_2Cl_2, then product **p-L** or **m-L** or **o-L** were filtered and obtain dry cake with 90% yield.

p-L: ^{1}H NMR (DMSO-d_6, 600 MHz): -3.05 (s, 2H, NH-H), 3.95 (s, 3H, -OCH_3-H), 4.70, 4.71 (d, J=6 Hz, 9H, -NCH_3-H), 7.63 (s, 1H, o-ph-H), 7.92 (s, 1H, o'-ph-H), 8.07 (s, 1H, b-ph-H), 8.11 (s, 1H, d-ph-H), 8.38 (s, 2H, a, e-ph-H), 8.73, 8.74 (d, J=6 Hz, 1H, CH=N-H), 8.97, 8.98 (d, J=6 Hz, 8H, β-pyrrole-H), 9.14, 9.16 (d, J=12 Hz, 6H, 3, 5 Py-H) 9.46 (s, 6H, 2, 6 Py-H). HRMS (ESI, positive ion mode, m/z): $[M]^{3+}$ calcd for $[C_{53}H_{42}N_9O_2]^{3+}$, 278.7815; found, 278.7805.

m-L: ^{1}H NMR (DMSO-d_6, 600 MHz): -3.03 (s, 2H, NH-H), 3.90 (s, 3H, -OCH_3-H), 4.73-4.74 (t, J_1=3.6 Hz, J_2=4.2 Hz, 9H, -NCH_3-H), 7.65 (s, 1H, o-ph-H), 7.93-7.96 (m, 1H, o'-ph-H), 8.09 (s, 1H, a-ph-H), 8.13 (s, 1H, c-ph-H), 8.40-8.45 (m, 1H, CH=N-H), 8.75, 8.76 (d, J=6 Hz, 2H, d, e-ph-H), 8.99-9.08 (m, 8H, β-pyrrole-H), 9.16-9.21 (m, 6H, 3, 5 Py-H), 9.48 (s, 6H, 2, 6 Py-H). HRMS (ESI, positive ion mode, m/z): $[M]^{3+}$ calcd for $[C_{53}H_{42}N_9O_2]^{3+}$, 278.7815; found, 278.7844.

o-L: ^{1}H NMR (DMSO-d_6, 600 MHz): -3.02 (s, 2H, NH-H), 3.91 (s, 3H, -OCH_3-H), 4.74 (d, J=3.6 Hz, 9H, -NCH_3-H), 7.94, 7.95, 7.96 (t, J_1=6 Hz, J_2=6 Hz, 1H,

CH=N-H), 8.10 (s, 1H, o-ph-H), 8.13 (m, 1H, o'-ph-H), 8.41-8.46 (m, 2H, b, c-ph-H), 8.76, 8.77 (d, J=6 Hz, 2H, d, e-ph-H), 8.99-9.09 (m, 8H, β-pyrrole-H), 9.19, 9.26 (br, 6H, 3, 5 Py-H), 9.49 (br, 6H, 2, 6 Py-H). HRMS (ESI, positive ion mode, m/z): $[M]^{3+}$ calcd for $[C_{53}H_{42}N_9O_2]^{3+}$, 278.7815; found, 278.7832.

1. 3. 4. Synthesis of p-CuP or m-CuP or o-CuP

The ligand **p-L** or **m-L** or **o-L** (100 mg, 0.12 mmol) and $CuCl_2 \cdot 2H_2O$ (5 equivalents) were added to 60 mL of MeOH at 60 ℃ for 6 h. The solvent was evaporated, the crude products were repetitive washed by ethyl acetate to give the complexes **p-CuP** or **m-CuP** or **o-CuP** as a dark purple solid. Yield: 90%.

p-CuP: Anal. Calcd for $C_{53}H_{41}Cl_4Cu_2N_9O_3$ (M_W: 1120.8551): C, 56.79; H, 3.69; N, 11.25; Found: C, 56.43; H, 3.92; N, 10.93. HRMS (ESI, positive ion mode, m/z): Calcd for $[M\text{-}3Cl]^{3+}$, 337.3865; Found, 337.3852.

m-CuP: Anal. Calcd for $C_{53}H_{41}Cl_4Cu_2N_9O_3$ (M_W: 1120.8551): C, 56.79; H, 3.69; N, 11.25; Found: C, 57.02; H, 3.46; N, 11.62. HRMS (ESI, positive ion mode, m/z): Calcd for $[M\text{-}3Cl]^{3+}$, 337.3865; Found, 337.3896.

o-CuP: Anal. Calcd for $C_{53}H_{41}Cl_4Cu_2N_9O_3$ (M_W: 1120.8551): C, 56.79; H, 3.69; N, 11.25; Found: C, 56.35; H, 4.03; N, 10.66. HRMS (ESI, positive ion mode, m/z): Calcd for $[M\text{-}3Cl]^{3+}$, 337.3865; Found, 337.3858.

The FTIR spectra of the complexes (**p-CuP**, **m-CuP** and **o-CuP**) and free ligands (**p-L**, **m-L** and **o-L**) are described in **Figure S4**, **S5** and **S6**. For free ligands, the in-plane bending vibration of the N-H (pyrrole rings) at 975, 974 and 974 cm^{-1} were observed. However, these bands disappeared in the spectra of **p-CuP**, **m-CuP** and **o-CuP** because of deprotonation and metalation of the pyrrole rings, besides, for complexes, the band at 433, 430 and 447 were attributed to characteristic peak of Cu-N coordination bonds and put it down to generated the metal complexes. Ligands show strong bands at 1633, 1632 and 1633 cm^{-1} due to $\nu_{(C=N),}$ but the complexes at 1624, 1623 and 1622 cm^{-1}, shifted to lower frequency has been observed. Together, these characteristic bands suggest that nitrogen atoms of the pyrrole rings and azomethine coordinate with metal ion [2-4].

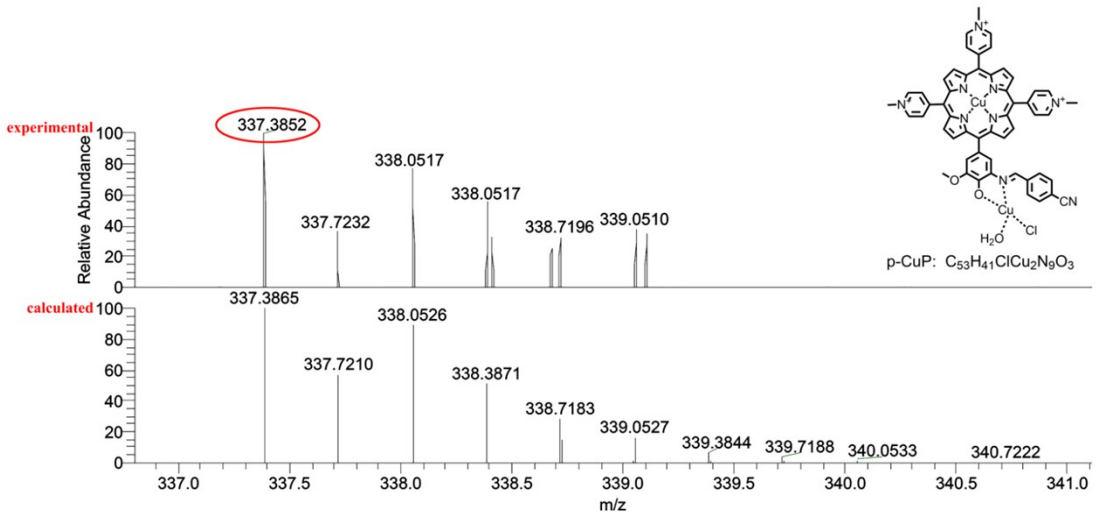

Figure S1. High resolution mass spectrum of p-CuP in CH_3OH: experimental and calculated spectra of the main peak.

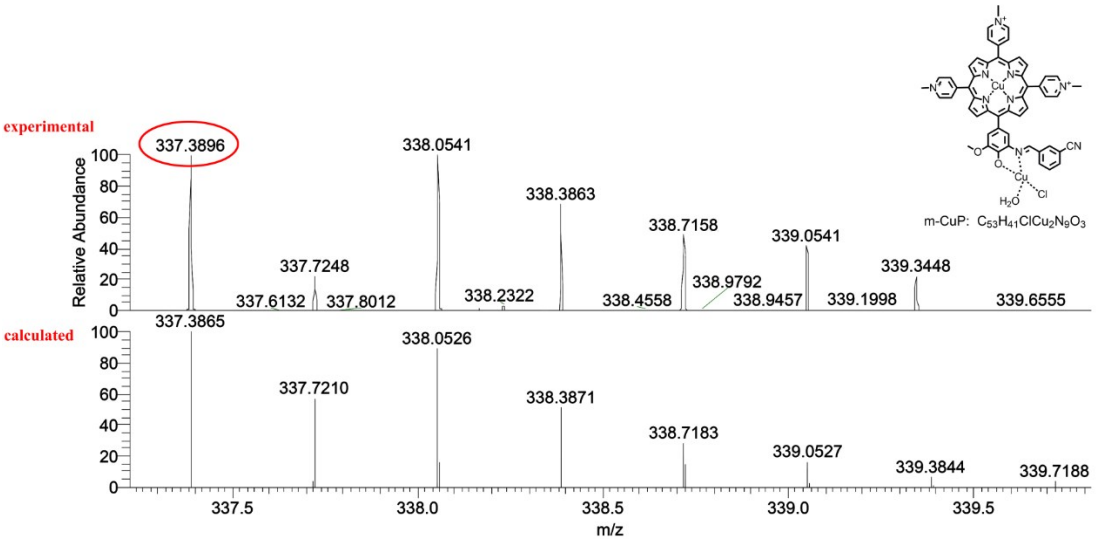

Figure S2. High resolution mass spectrum of m-CuP in CH_3OH: experimental and calculated spectra of the main peak.

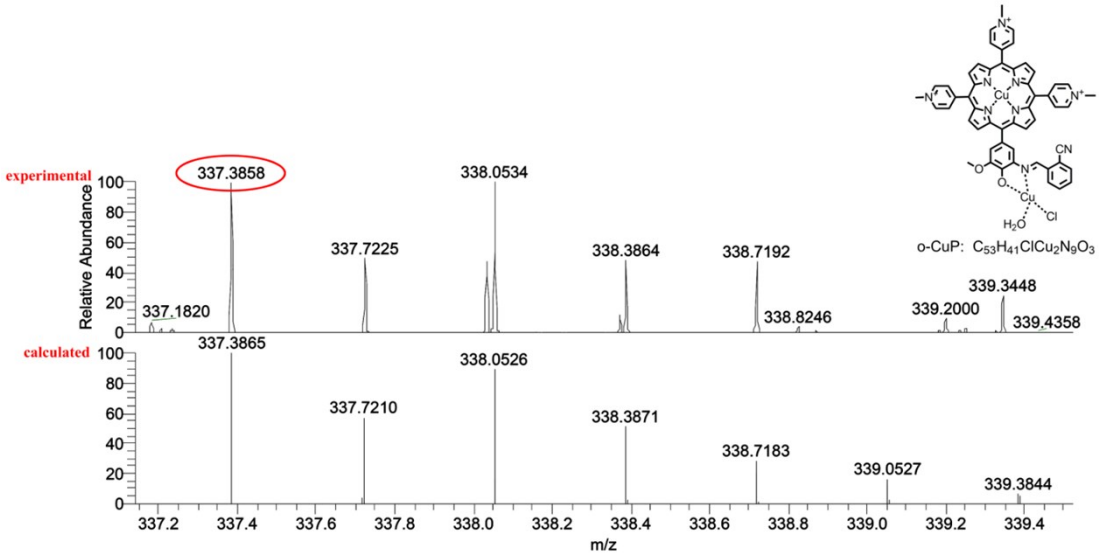

Figure S3. High resolution mass spectrum of o-CuP in CH_3OH: experimental and calculated spectra of the main peak.

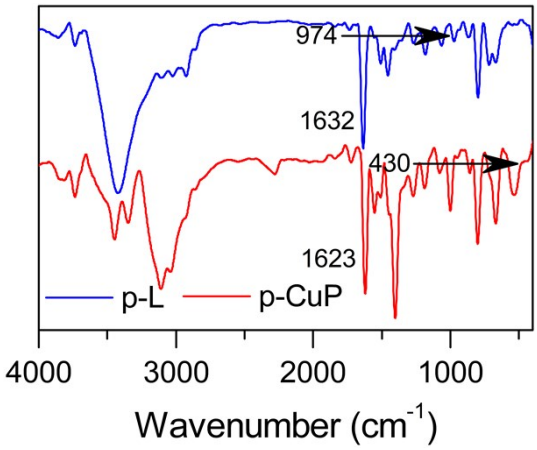

Figure S4. IR spectra of **p-L** and **p-CuP**.

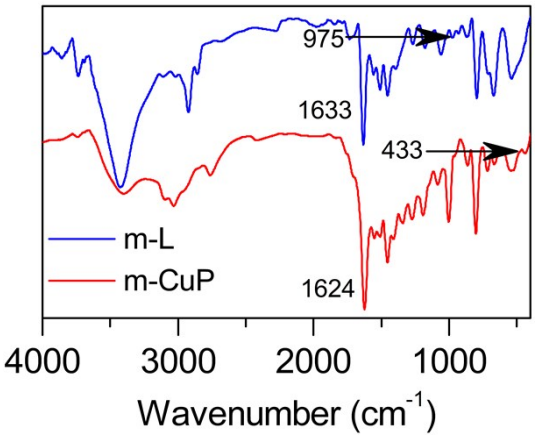

Figure S5. IR spectra of **m-L** and **m-CuP**.

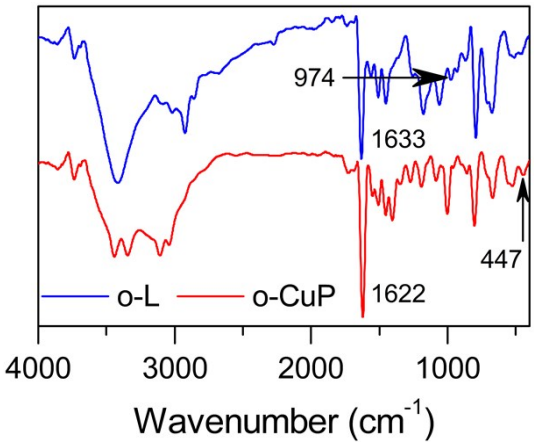

Figure S6. IR spectra of **o-L** and **o-CuP**.

2. Results and discussion

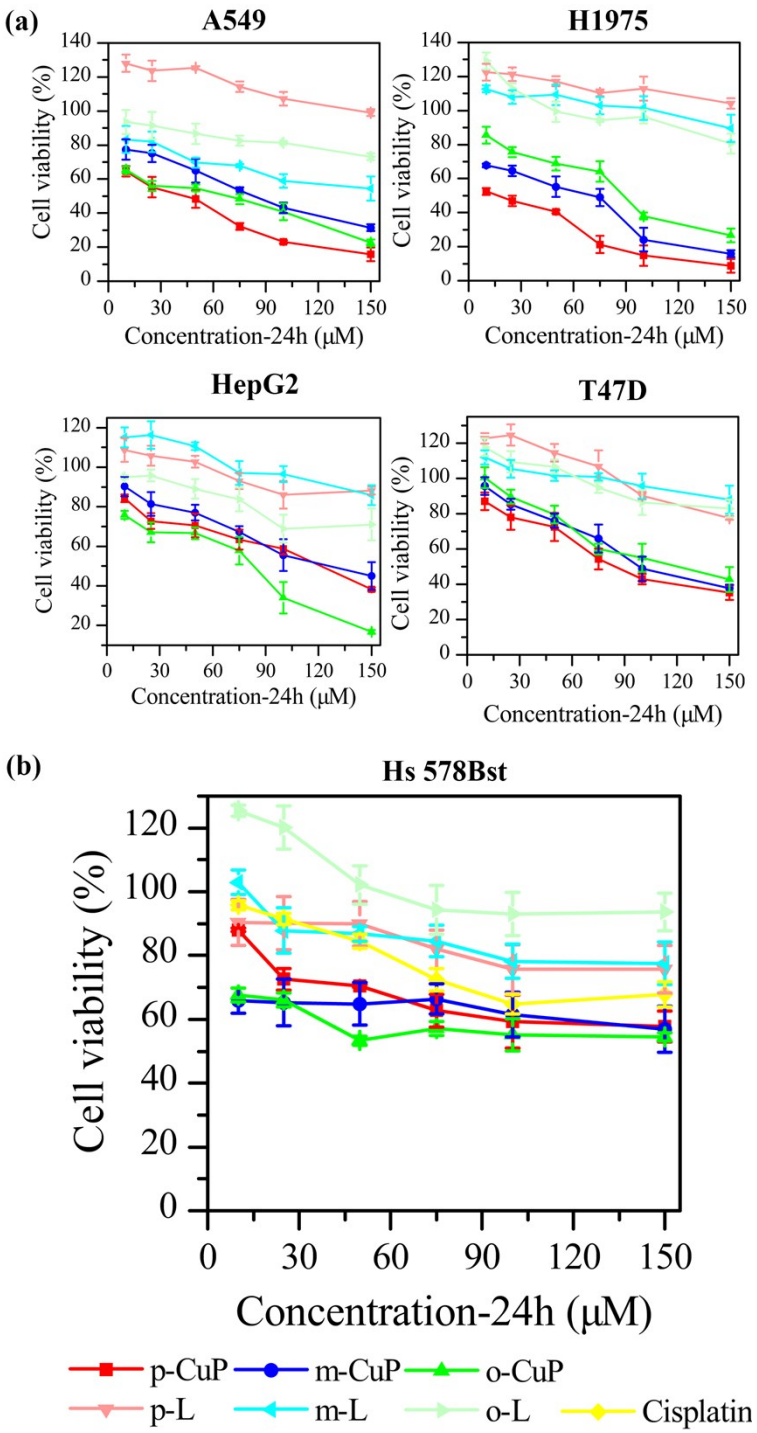

Figure S7. Ligands, complexes and cisplatin are being used in the treatment of **(a)** human cancer cell lines (A549, H1975, HepG2 and T47D), **(b)** normal cells (Hs 578Bst) for 24h.

Table S1. IC_{50} values (μM) of ligands, complexes and cisplatin with different cell lines for 24 h.

Compound	A549	H1975	HepG2	T47D	Hs 578Bst
p-CuP	28.309	16.464	126.656	88.45	＞150
m-CuP	77.108	40.618	139.45	106.774	＞150
o-CuP	42.545	80.112	58.91	115.566	＞150
p-L	＞150	＞150	＞150	＞150	＞150
m-L	＞150	＞150	＞150	＞150	＞150
o-L	＞150	＞150	＞150	＞150	＞150
Cisplatin	-	12.651	-	-	178.041

In Cisplatin row, "-" represents not determined

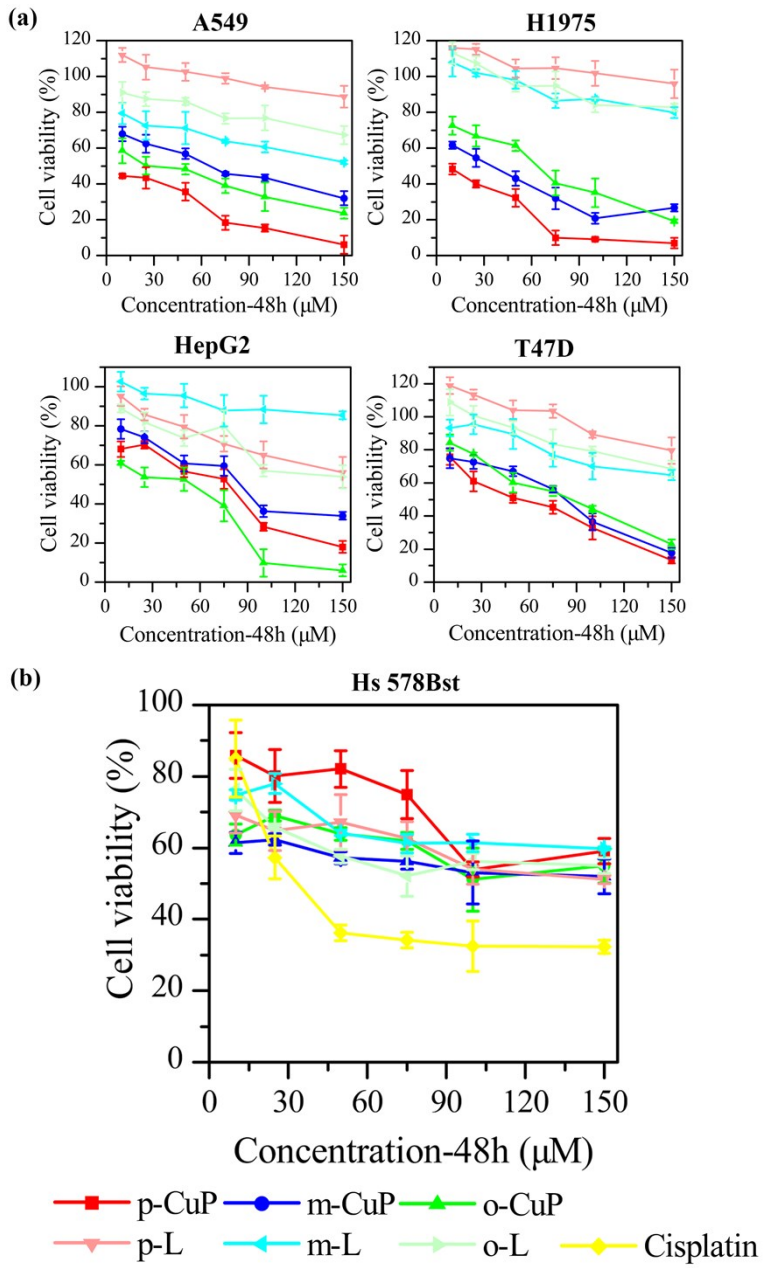

Figure S8. Ligands, complexes and cisplatin are being used in the treatment of (a) human cancer cell lines (A549, H1975, HepG2 and T47D), (b) normal cells (Hs 578Bst) for 48h.

Table S2. IC_{50} values (μM) of ligands, complexes and cisplatin with different cell lines for 48 h.

Compound	A549	H1975	HepG2	T47D	Hs 578Bst
p-CuP	8.3444	8.276	47.558	42.426	＞150
m-CuP	55.165	25.148	75.395	62.441	＞150
o-CuP	25.507	48.234	26.046	75.581	＞150
p-L	＞150	＞150	＞150	＞150	＞150
m-L	＞150	＞150	＞150	＞150	＞150
o-L	＞150	＞150	＞150	＞150	＞150
Cisplatin	-	4.085	-	-	55.638

In Cisplatin row, "-" represents not determined

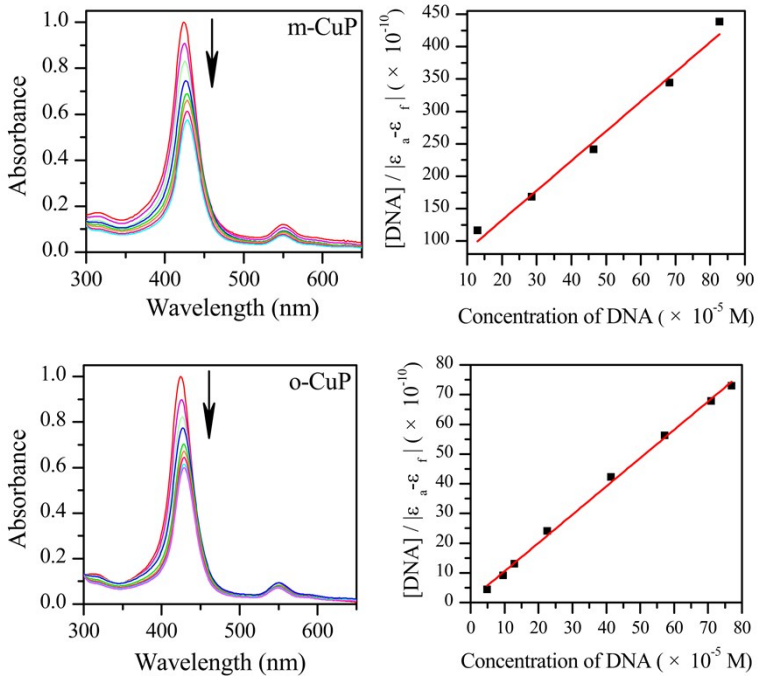

Figure S9. Absorption spectra of complex **m-CuP** and **o-CuP** in the presence ct-DNA at different concentrations (a) and (c). Calculation of binding constant (b) and (d).

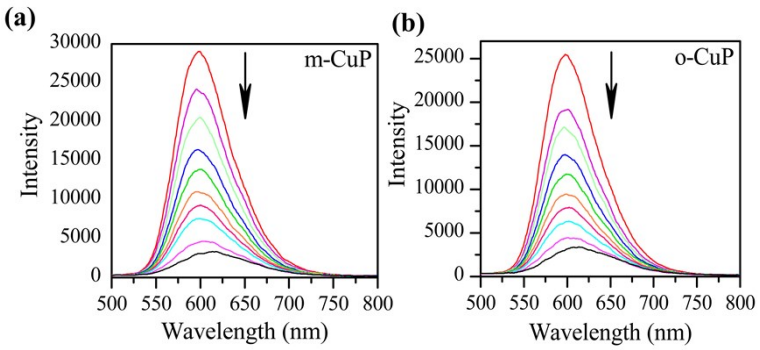

Figure S10. Fluorescence quenching of complex **m-CuP** and **o-CuP** bound to DNA-EtBr.

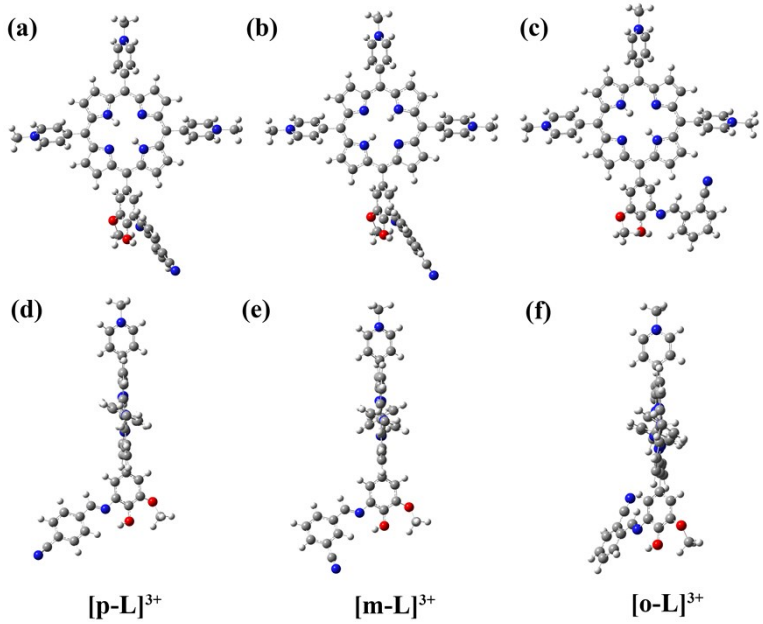

Figure S11. Optimized structures of cationic porphyrin ligands, top view (a) $[p\text{-}L]^{3+}$, (b) $[m\text{-}L]^{3+}$, (c) $[o\text{-}L]^{3+}$; side view (d) $[p\text{-}L]^{3+}$, (e) $[m\text{-}L]^{3+}$, (f) $[o\text{-}L]^{3+}$.

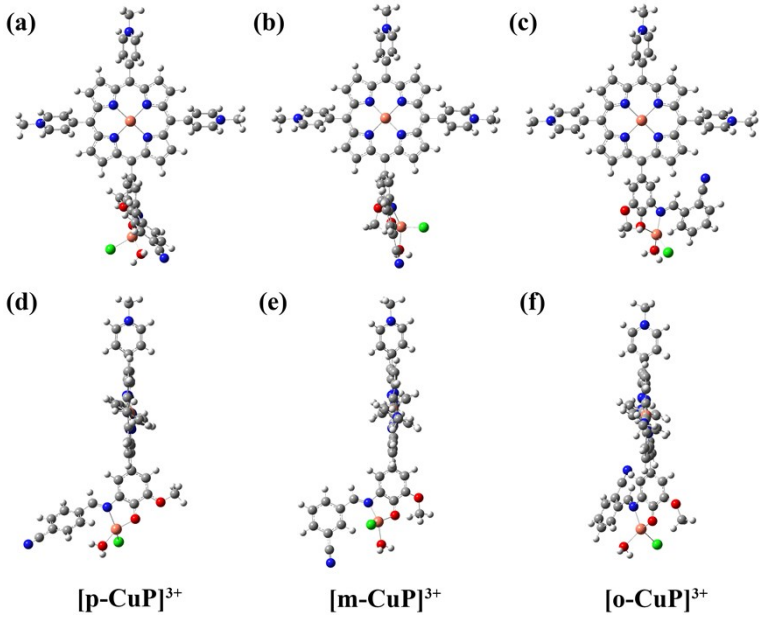

Figure S12. Optimized structures of cationic porphyrin complexes, top view (a) $[p\text{-}CuP]^{3+}$, (b) $[m\text{-}CuP]^{3+}$, (c) $[o\text{-}CuP]^{3+}$; side view (d) $[p\text{-}CuP]^{3+}$, (e) $[m\text{-}CuP]^{3+}$, (f) $[o\text{-}CuP]^{3+}$.

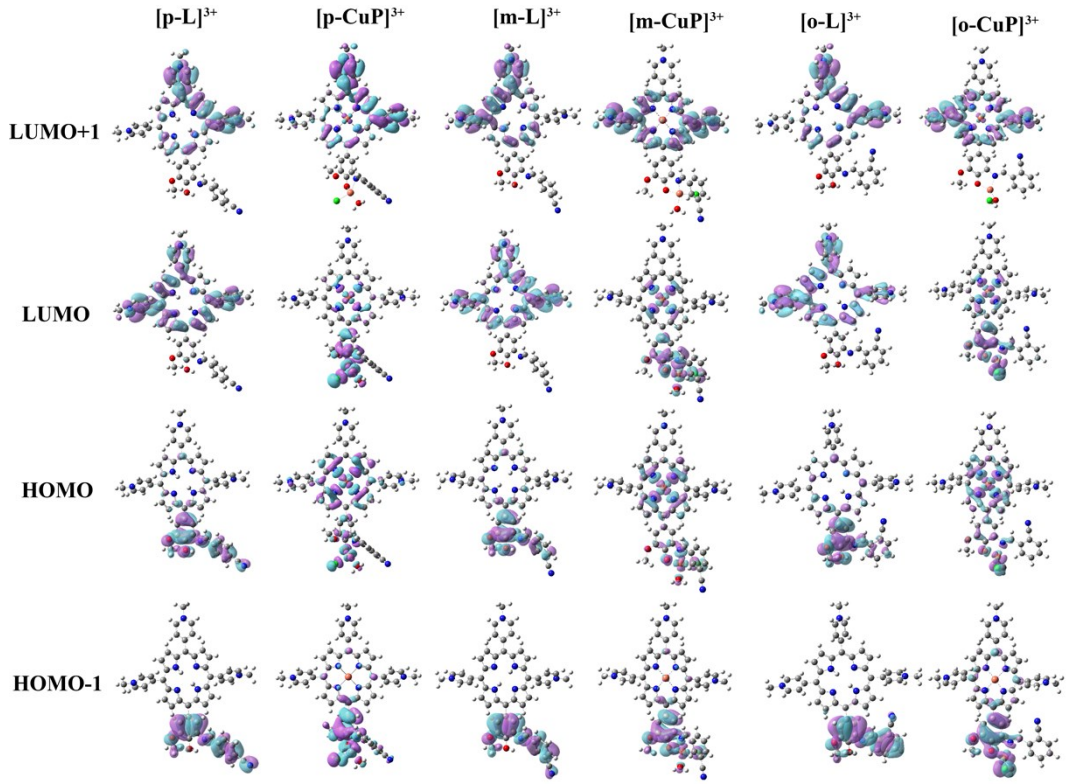

Figure S13. Frontier molecular orbitals for the HOMO-1, HOMO, LUMO, and LUMO+1, of the cationic porphyrin ligands and complexes.

Table S3. The calculated other parameters derived from HOMO, LUMO energy values.

Compound	E_{HOMO} (eV)	E_{LUMO} (eV)	ΔE^a (eV)	M^b	χ^c	η^d	S^e	ω^f
$[p\text{-}CuP]^{3+}$	-9.61324	-9.27882	0.334428	-9.44603	9.446029	0.167214	2.990179	266.8061
$[m\text{-}CuP]^{3+}$	-9.61079	-9.21324	0.397559	-9.41202	9.412015	0.198779	2.515353	222.8251
$[o\text{-}CuP]^{3+}$	-9.66685	-9.25269	0.414158	-9.45977	9.459771	0.207079	2.41454	216.0706

$I = -E_{HOMO}$, $A = -E_{LUMO}$;

$^a\Delta E = I - A$; $^b\mu = -(I + A) / 2$; $^c\chi = (I + A) / 2$; $^d\eta = (I - A) / 2$; $^eS = 1 / 2\eta$; $^f\omega = \mu^2 / 2\eta$.

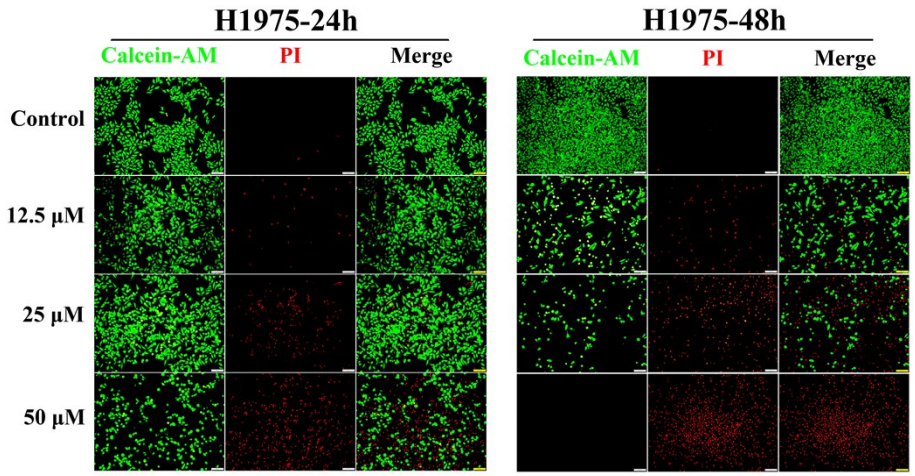

Figure S14. Fluorescent microscopic imaging of H1975 cells treated with **p-CuP** for 24 and 48h, by staining with Calcein-AM/propidium iodide (original magnification, 10×).

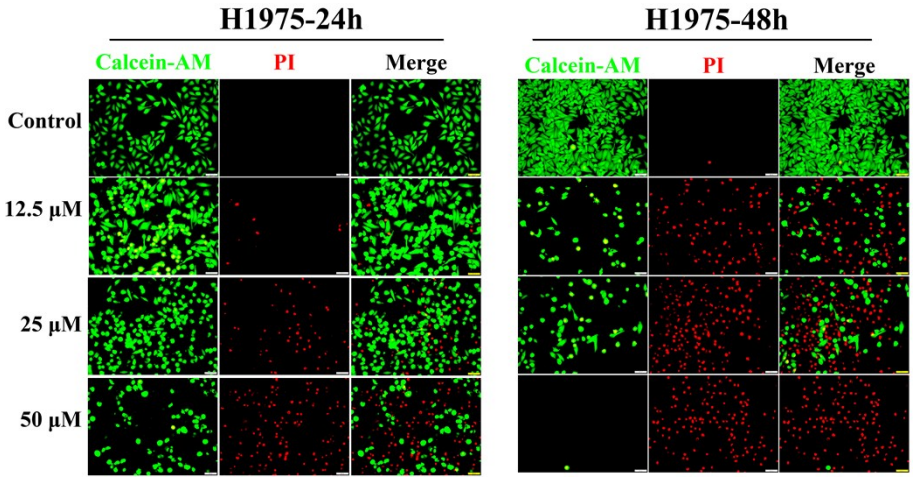

Figure S15. Fluorescent microscopic imaging of H1975 cells treated with **p-CuP** for 24 and 48h, by staining with Calcein-AM/propidium iodide (original magnification, 20×).

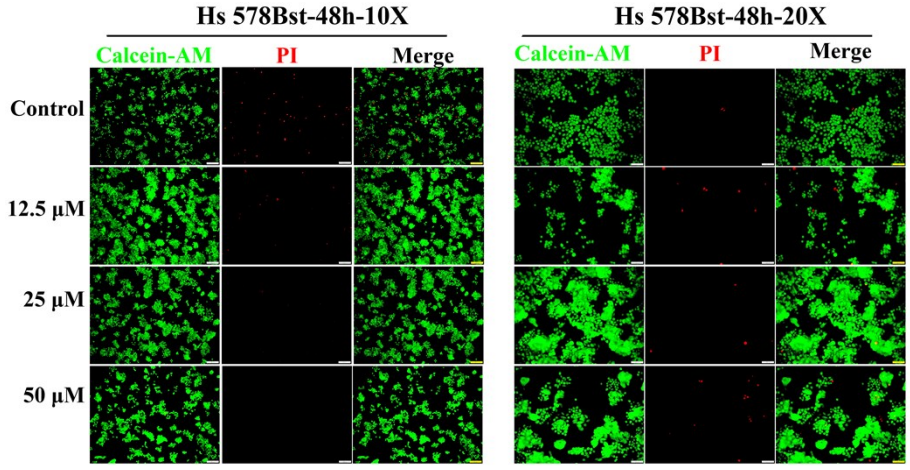

Figure S16. Fluorescent microscopic imaging of Hs 578Bst cells treated with **p-CuP** for 48h, by staining with Calcein-AM/propidium iodide (original magnification, 10 and 20×).

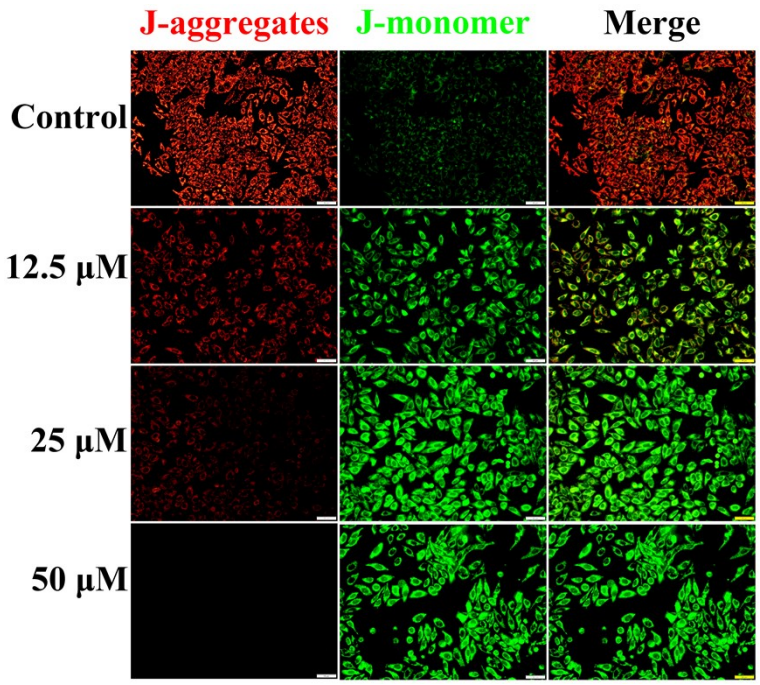

Figure S17. The mitochondrial membrane potentials (MMPs) using JC-1 after staining H1975 cellss with **p-CuP** observed by fluorescence microscope (original magnification, 10×)

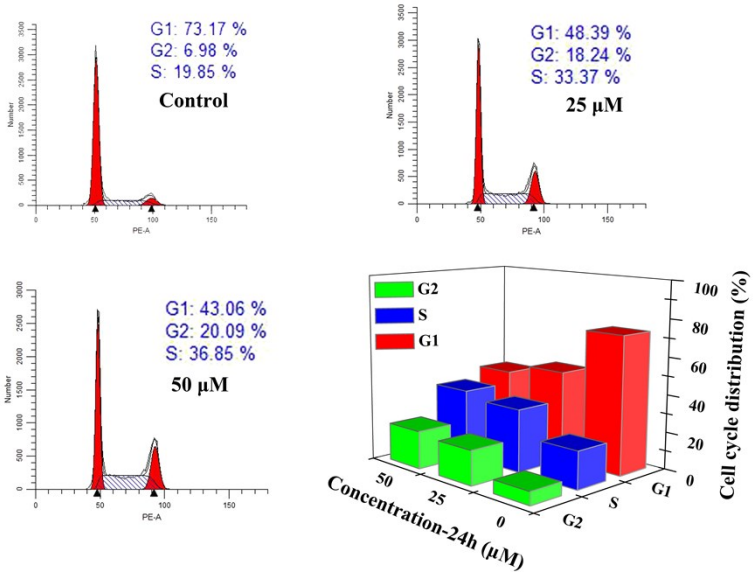

Figure S18. Cell cycle arrest of complex **p-CuP** against H1975 cells after 24h.

References

1. Q. Zhang, Q. Zhang, Z.-z. Li, H. Liu and J.-c. Liu, *Dyes Pigment.*, 2020, **173**, 107923.
2. R. Boscencu, *Molecules*, 2011, **16**, 5604-5617.
3. W. Chen, M. E. El-Khouly and S. Fukuzumi, *Inorg. Chem.*, 2011, **50**, 671-678.
4. Y.-F. Huo, L.-N. Zhu, K.-K. Liu, L.-N. Zhang, R. Zhang and D.-M. Kong, *Inorg. Chem.*, 2017, **56**, 6330-6342.